



## Uranium - Doping Effects on Structural & Spectral Features of Vanadate Ceramics

**Khaled M. Elsabawy<sup>a,b</sup>**

<sup>a</sup>Materials Science Unit, Chemistry Department, Faculty of Science,  
Tanta University, 31725 - Tanta, Egypt

<sup>b</sup>Department of Chemistry, Faculty of Science, Taif University,  
Taif city, Alhawayah - 888, Saudi Arabia

Phone: +9660503252190

E-mail address: [khaledelsabawy@yahoo.com](mailto:khaledelsabawy@yahoo.com) , [ksabawy@yahoo.com](mailto:ksabawy@yahoo.com)

### ABSTRACT

212-Vanadate ceramics with formula  $\text{Bi}_2\text{SrV}_{2-x}\text{U}_x\text{O}_9$ , where ( $0 \leq x \leq 0.6$  mole) were carefully synthesized by solution routes with sintering temperature at 88 °C for 24 hrs. Structural analysis with XRD proved that uranium (IV)-dopant can substitute successfully until  $x = 0.55$  mole on the Bi-layered perovskite crystal structure without damaging the original structure. It was observed that U – doping have slight to moderate effects on both ESR-signals and conduction mechanism of U-doped Bi-Sr-V-O regime. Electrical measurements indicated that the energy gap  $E_g$  and number of electrons in conduction band  $N_{cb}$  increase as the ratio of U doping increases from  $x = 0.05$  till  $x = 0.6$  mole respectively due to the increasing of paramagnetic character of uranium than vanadium.

**Keywords:** 212 Vanadate, Uranium Doping, Ceramic, X- ray, ESR, IR

### 1. INTRODUCTION

The 212-Bi-Sr-V-O have attracted increasing attention in the research community because they are fatigue – free and lead free [1-3]. The wide spread application and

commercialization of bismuth- layered perovskite ferroelectrics have been limited by drawbacks, their rather high processing temperature and their relatively low remanent polarization [4-5]. Recently, efforts have been made to enhance the properties of layered perovskite ferroelectrics by addition or substitution of alternative cations [6-8]. It's now well established that the variation of oxygen content and distribution of oxygen atoms on the lattice site strongly influences the physical and structural properties (e.g. electrical conductivity) at high-temperature. Superconductors and many other metallic oxides [9].

The discovery of high temperature superconductors has attracted much attention for their technological application such as superconducting quantum interference devices (SQUID), The high T<sub>c</sub> ceramic super-conductor, the Bi –based system has been studied because of its high critical temperature especially with the partial substitution of Pb in Bi and Sr sites since it promotes the stabilization of 2223 phase when grown from 2212 phase [10-11].

Many published papers [12-14] are explaining the discovery of mixed metal oxides having bismuth layer alternating with perovskite structure layers, because of their ionic structural framework, Aurivillius phases exhibit great flexibility with respect to metal cation substitution. Therefore, these phases have high potential for systematic control of their properties [15].

There are different studies showing the chemical substitution such as Pb doping on Bi-O layers that can be used to improve conduction in the blocking layers and so to a large decrease in the resistivity anisotropy. The reduced anisotropy leads to improvement of the critical current in the heavy Pb-doped [16-21].

Das et al. [22] reported the improved remanent polarization of SBN and SrBi<sub>2</sub>Ta<sub>2</sub>O<sub>9</sub> this films, when a small amount of Ca cations were incorporated into A sites: Bismuth layered perovskite materials have high fatigue resistance [23, 24].

The crystal structure and chemical composition of these layered perovskites were systematically studied [25] with the general formula of (Bi<sub>2</sub>O<sub>2</sub>)<sup>2+</sup> (Am<sup>-1</sup>BmO<sup>3m+1</sup>)<sup>3-</sup>, consisting of m-perovskite unites sandwiched between bismuth oxide layers called the family of bismuth layered structured ferroelectrics [26], where A and B two types of cations that enter the perovskite unite A is Bi<sup>3+</sup>, Ba<sup>2+</sup>, Sr<sup>2+</sup>, and B is Ti<sup>4+</sup>, Ta<sup>5+</sup>, and m = 1-6 layered perovskite strontium tantalite is a member of bismuth layer- structured ferroelectrics.

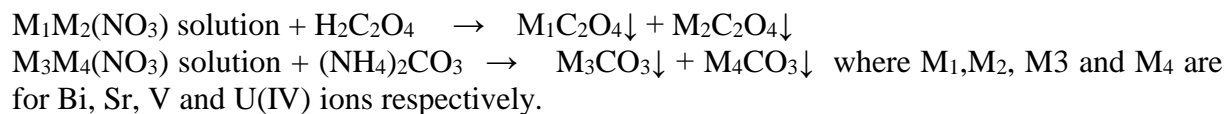
The crystal structure of SrBi<sub>2</sub>Ta<sub>2</sub>O<sub>9</sub> comprises pseudo- perovskite blocks (SrTa<sub>2</sub>O<sub>7</sub>)<sup>2-</sup> that are sandwiched between (Bi<sub>2</sub>O<sub>2</sub>)<sup>2+</sup> layers. Sr occupies the A site of the perovskite block and Ta occupies the B-site [27].

The essential goal of the present investigations is to investigate effects of wide range of U – dopings on vanadium-sites on the main structural, electrical and spectroscopic features of 212-perovskite vanadate ceramics.

## **2. EXPERIMENTAL**

The pure perovskite Bi<sub>2</sub>SrV<sub>2</sub>O<sub>9</sub> and different U-doped samples with the general formula Bi<sub>2</sub>SrV<sub>2-x</sub>U<sub>x</sub>O<sub>9</sub>, where x = 0.05, 0.1, 0.2, 0.3, 0.6 mole were prepared by conventional solid state reaction and solution routes with sintering procedure using the appropriate amounts of Bi<sub>2</sub>(CO<sub>3</sub>)<sub>3</sub>, SrCO<sub>3</sub>, (NH<sub>4</sub>)<sub>2</sub>VO<sub>3</sub> and UO<sub>2</sub> (each purity > 99%).

Uranium oxide is tested by Gieger counter of radioactivity it was radioactive oxide with low emission. The mixture was ground in an agate mortar for one hour then dissolved in few drops of concentrated nitric acid then dilution process was made with adjusting pH-value by 30% ammonia solution. The obtained solution was divided into two portion and one portion was treated by 0.4M oxalic acid and the other one by ammonium carbonate 0.4M respectively.



The result metals precipitates ( as oxalates and carbonates ) were collected and dried in oven at 80 °C .Then the finely ground powder was subject to firing at 800 °C for 10 hours, reground and finally pressed into pellets with thickness 0.2 cm, diameter 1.2 cm and sintered at 880 °C for 24 hours. Then the furnace is cooled slowly down to room temperature. Finally the materials are kept in vacuum desiccator over silica gel dryer.

## **2. 1. Structural Measurements**

### **2. 1. 1. X-Ray diffraction (XRD)**

The X-ray diffraction measurements (XRD) were carried out at room temperature on the fine ground  $Bi_2SrV_2O_9$  and  $Bi_2SrV_{2-x}U_xO_9$  systems in the range ( $2\theta = 10-80^\circ$ ) using Cu-K $\alpha$  radiation source and a computerized [Bruker Axs-D8 advance] X-ray diffractometer with two theta scan technique.

### **2. 1. 2. Conductivity Measurements**

The DC-electrical conductivity of the samples was measured using the two terminals DC-method. The pellets were inserted between spring loaded copper electrodes, A KEITHLEY 175 multimeter (ASA) was employed from room temperature up to 500 K. The temperature was measured by a calibrated chromel-alumel thermocouple placed firmly at the sample. Measurements were conducted in such a way that at each temperature, sufficient time was allowed to attain thermal equilibration.

### **2. 1. 3. Solid infrared absorption spectral measurements**

The IR absorption spectra of the prepared samples were recorded using "Nexus 670 FT IR spectrometer in the range 500-2500  $cm^{-1}$  using pure KBr matrix".

### **2. 1. 4. Electron paramagnetic resonance measurements**

The electron spin resonance spectra (ESR) were recorded at room temperature for the prepared samples using at x-band frequencies on a "Bruker- ELEXSYS E 500 Germany" spectrometer.

## **3. RESULTS & DISCUSSION**

### **3. 1. X-Ray Diffraction**

The X-ray diffraction patterns of pure and variant U-doped samples with the general formula  $\text{Bi}_2\text{SrV}_{2-x}\text{U}_x\text{O}_9$ , where  $x = 0.05, 0.1, 0.2, 0.3, 0.6$  mole are shown in Fig (1a-f). Analysis of the corresponding  $2\theta$  values and the interplanar spacing  $d(\text{\AA})$  by using computerized program proved that the compound is mainly belongs to distorted perovskite type with hexagonal crystal form, that expressed by assigned peaks in major. The unite cell dimensions were calculated using parameters of the most intense X-ray reflection peaks and found to be  $a = b = 5.7984 \text{ \AA}$  and  $c = 7.2124 \text{ \AA}$  for the pure  $212\text{Bi-Sr-V-O}$ . Single phase of the layered perovskite structure appeared when  $M^{4+}$  is up to or equal 0.05 [28]. The substitution of  $\text{U}^{4+}$  for  $\text{V}^{5+}$  in BSV would induce A-site cation vacancies in perovskite layers, which leads to an increase of internal stress for the shrinkage of unite cell volume as reported in [29]. The increasing of tetravalent thorium ions in the crystal lattice of BSV will result in strong stress, which will expel other U -ions from the crystal lattice of BSV( $212\text{-Bi-V-O}$ ) causing some extent of distortion on the perovskite layers.

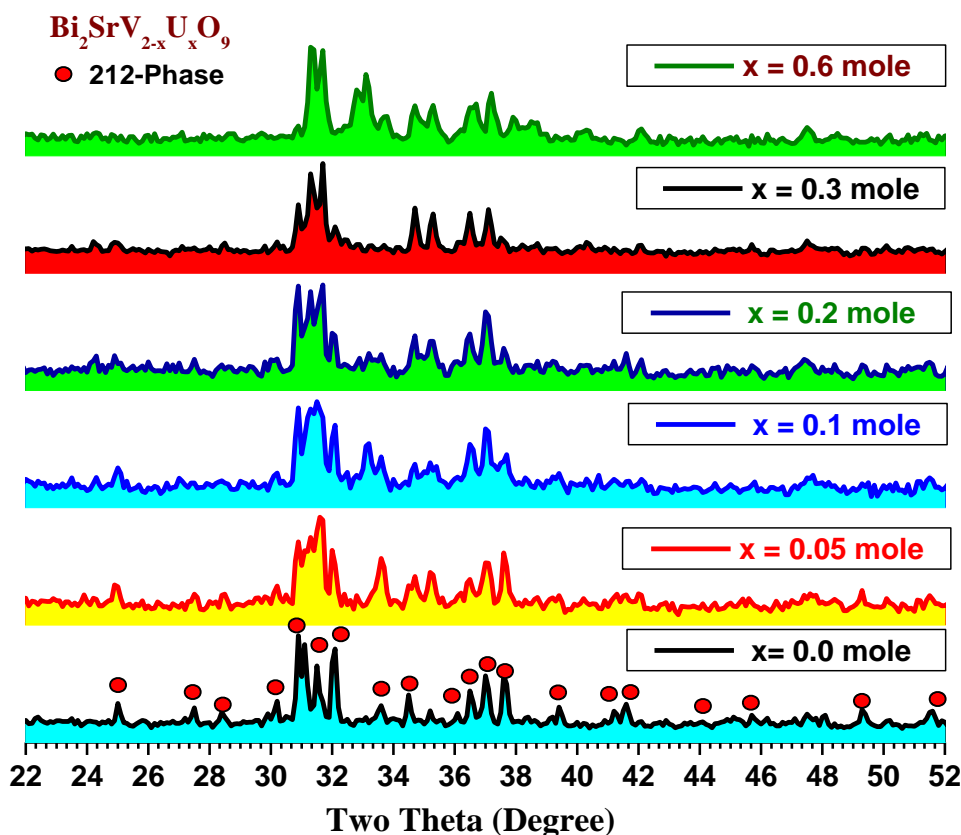


**Fig. 1(a-f).** XRD patterns recorded for: (a) - pure  $\text{Bi}_2\text{SrV}_2\text{O}_9$  and U-doped samples; (b) -  $\text{Bi}_2\text{SrV}_{1.95}\text{U}_{0.05}\text{O}_9$ ; (c) -  $\text{Bi}_2\text{SrV}_{1.9}\text{U}_{0.1}\text{O}_9$ ; (d) -  $\text{Bi}_2\text{SrV}_{1.8}\text{U}_{0.2}\text{O}_9$ ; (e) -  $\text{Bi}_2\text{SrV}_{1.7}\text{U}_{0.3}\text{O}_9$ ; (f) -  $\text{Bi}_2\text{SrV}_{1.4}\text{U}_{0.6}\text{O}_9$

The layered perovskite structure would be more restrictive since  $(\text{Bi}_2\text{O}_2)^{2+}$  interlayeres impose a great constraint for structural relaxation. Such a structural constraint induced from

$(\text{Bi}_2\text{O}_2)^{2+}$  interlayeres may well explain the lack of an appreciable decrease in lattice parameters with an increased amount of vanadium doping [30].

From Fig. (2) It is clear that *c-axis* increases as result of substitution U- dopant on the bases of ionic radius it is expected that *c-axis* increases as  $\text{U}^{4+}$  doping ratio increases. Furthermore,  $\text{U}^{4+}$  is lower in charge than  $\text{V}^{5+}$  and as a result it is expected to decrease stress inside lattice and consequently the shrinkage factor of lattice will be increased. From Fig. (1a-f). It is clear that the U- substitutions are successful in the most of investigated range even at high concentration  $x = 0.6$  mole since there is no evidence noticeable at X-ray diffractogram referring to U- impurity phase which reflects that all doping ratios are within the internal lattice structure. This confirms that U-dopant can substitute in the V-sites successfully in the whole investigated range.

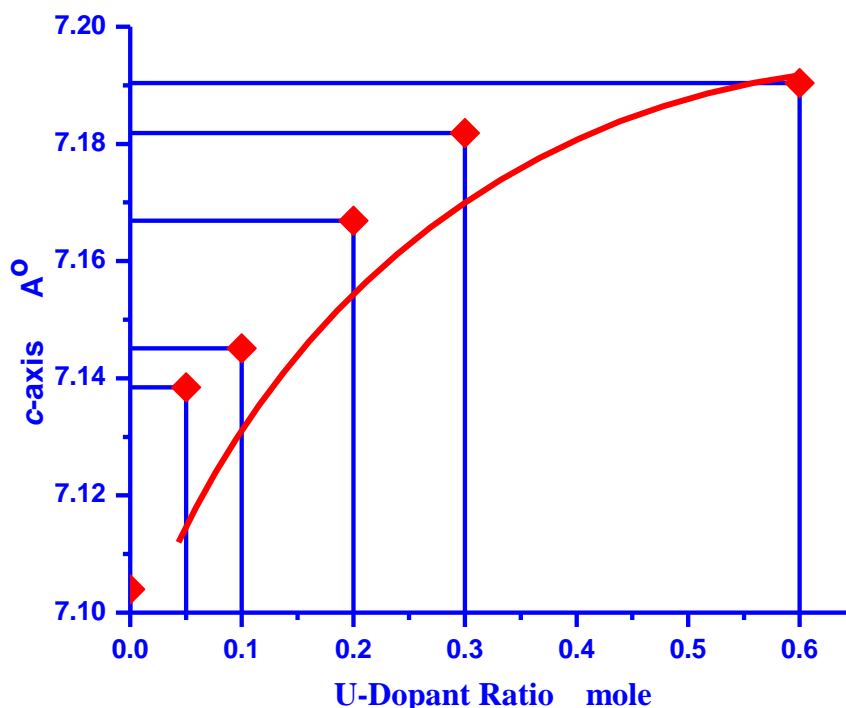


**Fig. 2.** Variation of *c-axis* as a function of U-content.

### 3. 2. Electron paramagnetic resonance measurements

Fig (3a,c,e) explain the electron spin resonance (ESR) signals recorded for pure Bi-212-vanadates and some selected uranium doped samples with  $x = 0.1, 0.3$  mole.

It was shown that the effective *g*-values ( $g_{\text{iso}}$ ) exhibit an increase from  $x = 0.0$  mole to  $x = 0.3$  mol due to strong interaction of coupling between  $\text{U}^{4+}$  ion that substitutes  $\text{V}^{5+}$  ion successfully at low dopant concentration as shown in Fig. (4).

These results of ESR-spectra proved that the anisotropy occurred as a result of increasing of U- doping is due to the increasing of paramagnetic character of substituted vanadates where  $g_{\text{eff}}$  varies as function of  $x$  value [31-32].

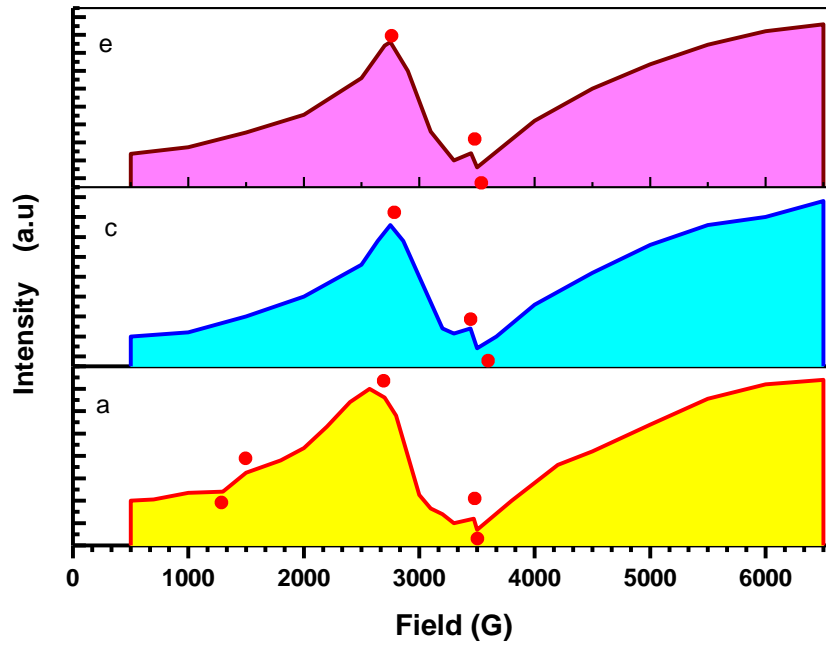


**Fig. 3(a,c,e).** ESR spectra at room temperature for pure and some selected U-doped 212-Bi-Sr-V-O system where (a):  $\text{Bi}_2\text{SrV}_2\text{O}_9$ , (c):  $\text{Bi}_2\text{SrV}_{1.9}\text{U}_{0.1}\text{O}_9$  and (e):  $\text{Bi}_2\text{SrV}_{1.7}\text{U}_{0.3}\text{O}_9$

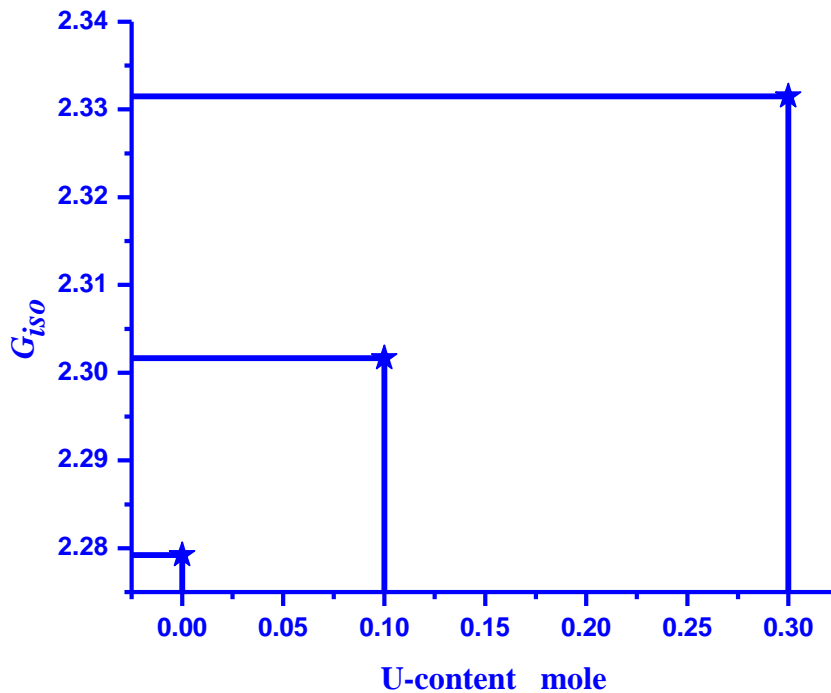


**Fig. 4.** Variation of  $G_{180}$  versus U-content.

**3. 3. DC-Electrical conductivity measurements**

Fig. (5a-f) displays the variation of DC-electrical conductivity as a function of reciprocal of absolute temperature for various U<sup>4+</sup> dopings. The data from Fig. (5a-f) exhibit conducting and semiconductor behavior since the conductivity increases as the temperature rise in case of conductor and the conductivity decrease as the temperature rise in case of semiconductor. [33].

Fig. (6a,b) show the relation between the energy gap (E<sub>g</sub>), number of e<sup>-</sup> in conduction band (N<sub>cb</sub>) for U- doped samples in which both of E<sub>g</sub> and N<sub>cb</sub> increase as the ratio of U - doping increases from x = 0.05 till x = 0.6 mole which may attributable to the numbers of unpaired electrons in the thorium outer shell is higher than those existed in the vanadium ions.

$$\rho = \rho_0 e^{-\Delta E_g/KT} \dots\dots\dots (Eq. 1)$$

$$N_{cb} = AT^{3/2} e^{-E_g/2KT} \dots\dots\dots (Eq. 2)$$

where: A = constant, E<sub>g</sub> = Energy gap in eV, K = Boltzmann constant and finally N<sub>c</sub> = numbers of electrons in the conduction band in electrons unit.

Further more the energy gap in the thorium band structure is lower than vanadium and as result number of electrons evaluated in the conduction band N<sub>c</sub> are increase as thorium dopings increase.

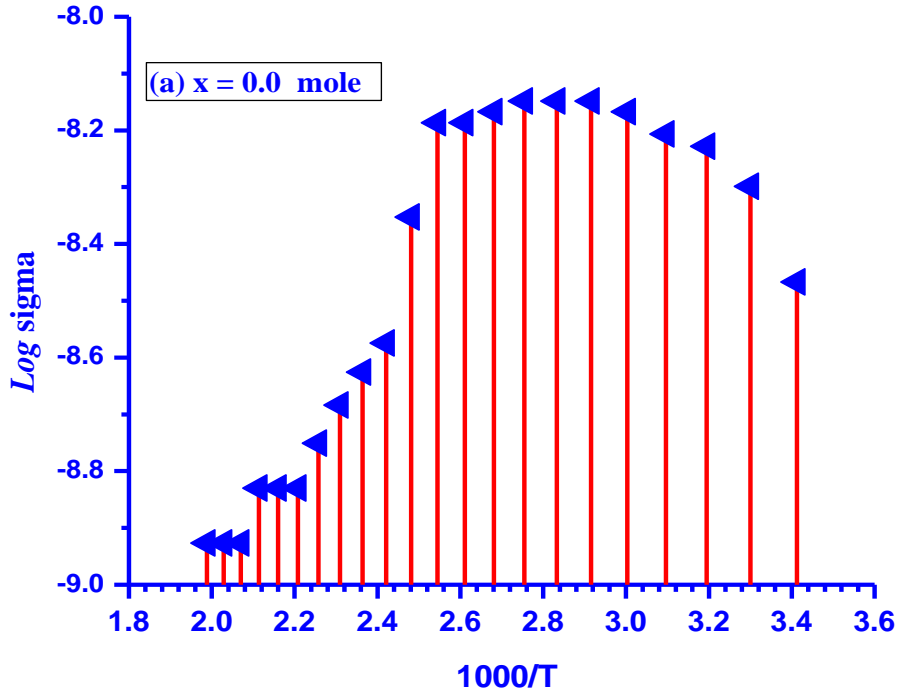


**Fig. 5(a).** Variation of DC- electrical conductivity as a function of temperature for pure 212-Bi-Sr-V-O system.

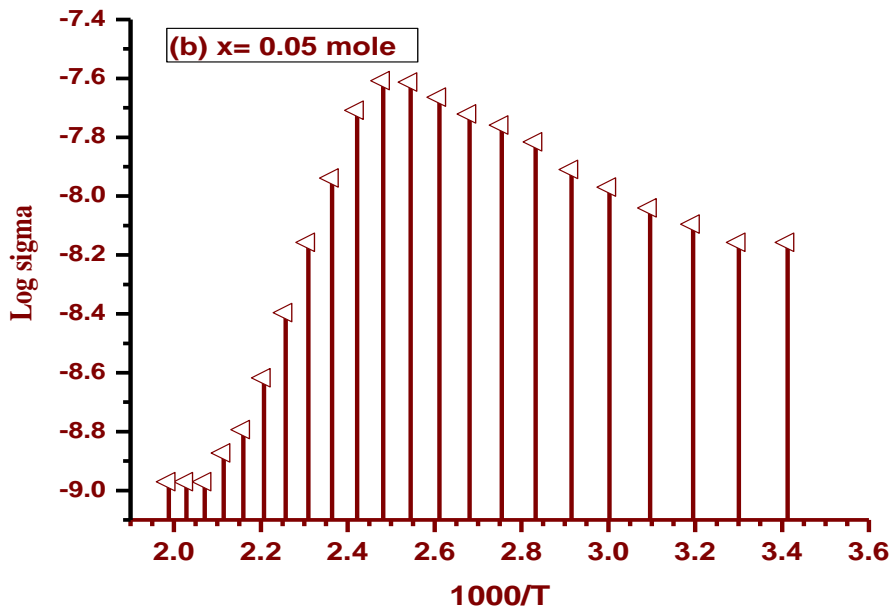


Fig. 5(b). Variation of DC- electrical conductivity as a function of temperature for (b)  $\text{Bi}_2\text{SrV}_{1.95}\text{U}_{0.05}\text{O}_9$

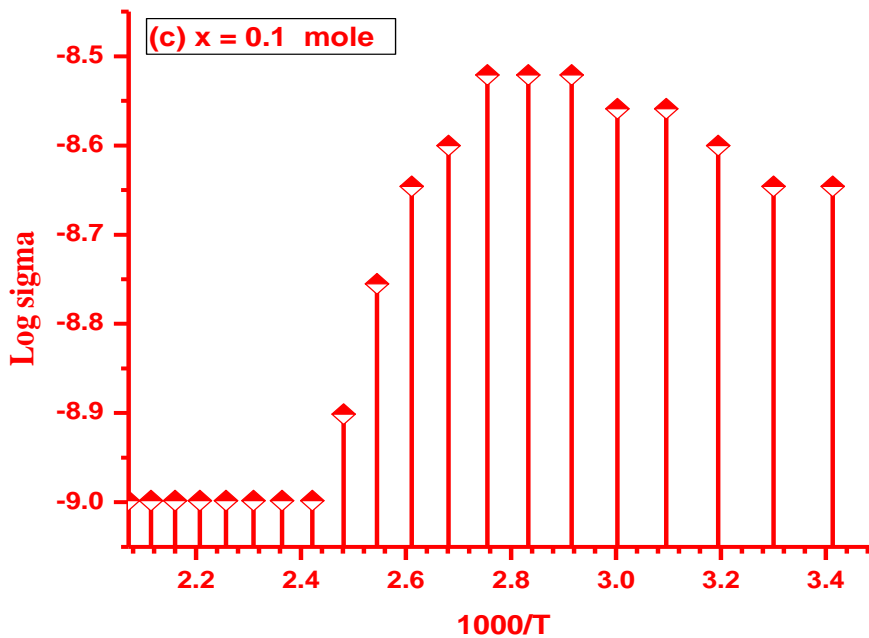


Fig. 5(c). Variation of DC- electrical conductivity as a function of temperature for (c)  $\text{Bi}_2\text{SrV}_{1.9}\text{U}_{0.1}\text{O}_9$ .

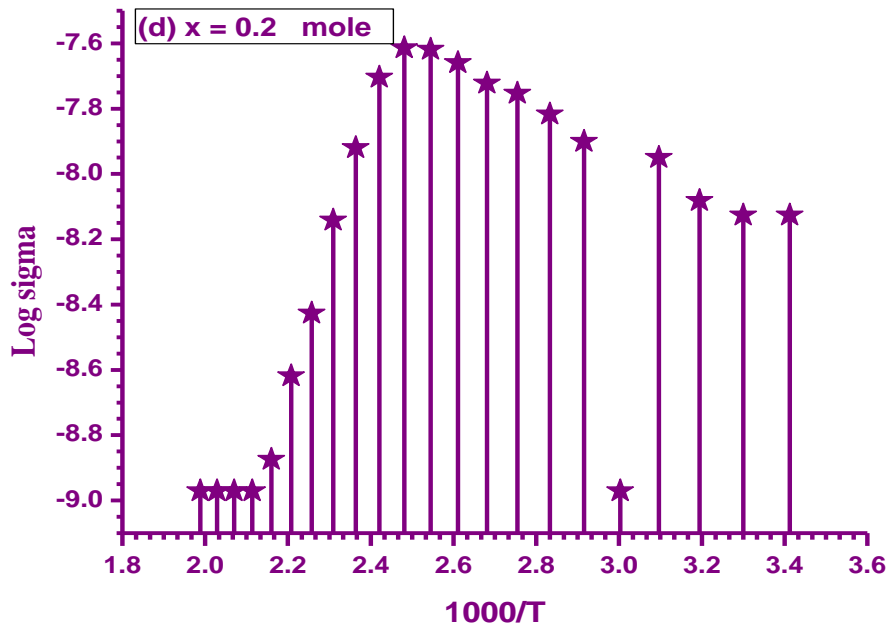


Fig. 5(d). Variation of DC- electrical conductivity as a function of temperature for (d)  $\text{Bi}_2\text{SrV}_{1.8}\text{U}_{0.2}\text{O}_9$ .

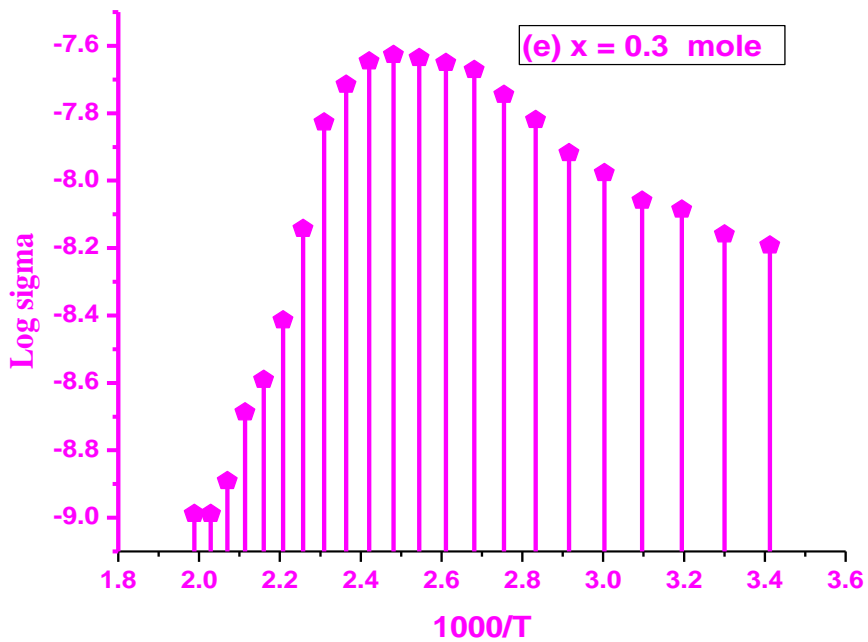


Fig. 5(e). Variation of DC- electrical conductivity as a function of temperature for (e)  $\text{Bi}_2\text{SrV}_{1.7}\text{U}_{0.3}\text{O}_9$ .

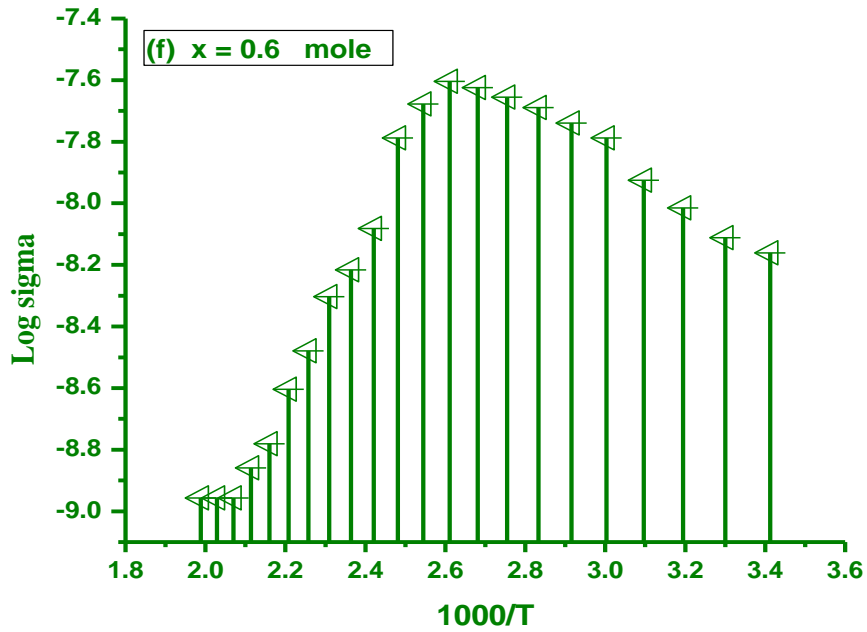


Fig. 5(f). The variation of DC- electrical conductivity as a function of temperature for (f)  $\text{Bi}_2\text{SrV}_{1.6}\text{U}_{0.4}\text{O}_9$ .

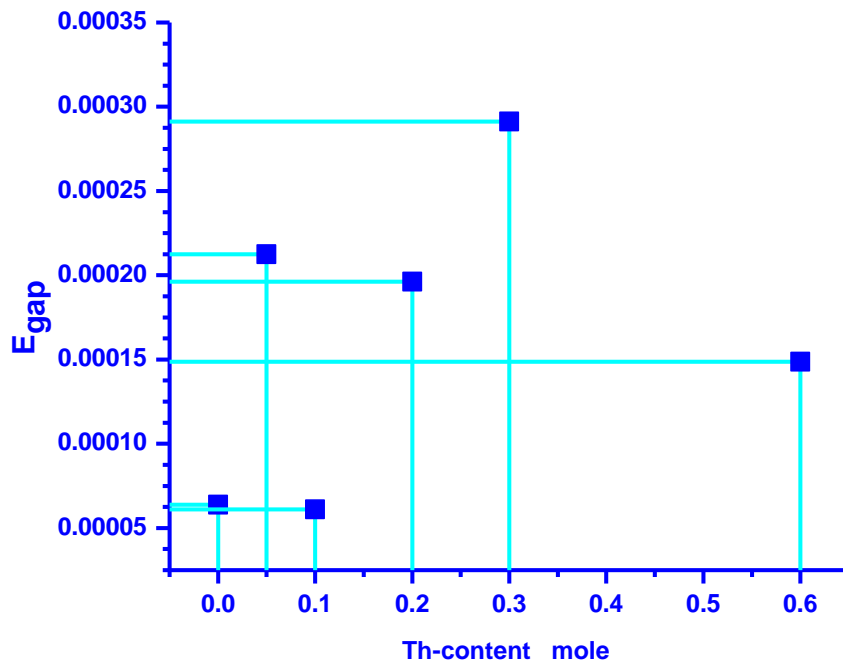


Fig. 6(a). Variation of  $E_{\text{gap}}$  versus U-content.

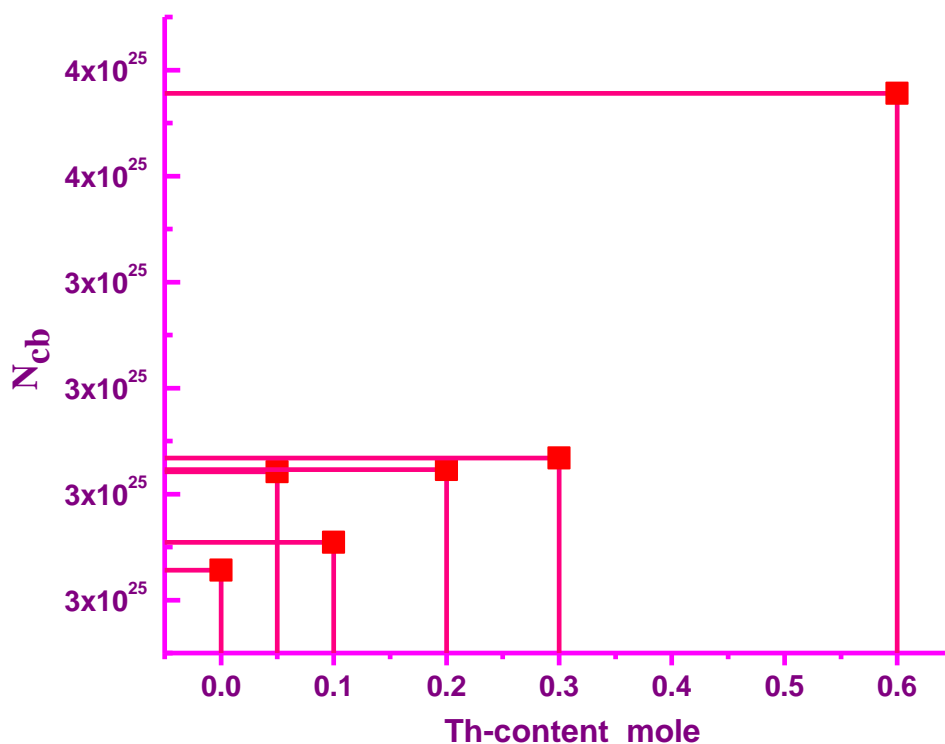


Fig. 6(b). Variation of  $N_{cb}$  versus U –content.

### 3. 4. Solid infrared absorption spectral measurements

The infrared absorption spectra of pure  $\text{Bi}_2\text{SrV}_2\text{O}_9$  and their uranium doped in the range of  $500\text{-}2500\text{ cm}^{-1}$  are shown in Fig. (7).

It is well known that  $212\text{-Bi-Sr-V-O}_9 \pm \delta$  system is mainly belongs to deficient perovskite structure and extra oxygen atom ( $\text{O}_9 \pm \delta$ ). Oxygen nine converts it to distorted perovskite structure and consequently the common vibrational modes of IR-spectra of perovskite are clearly appear.

From Fig. (7), we can summarize the different vibrational modes and their reasons as follows;

- (a): The range from  $390\text{-}620\text{ cm}^{-1}$  includes the most of infrared active phonons involving stretching modes of vibrating Bi-O, Sr-O and V-O/U-O plus bending modes of Bi-O-V, Bi-O-Sr, respectively.
- (b): The broad band around  $800\text{ cm}^{-1}$  is mainly due to an increase in the free carrier scattering as reported in many previously published papers as reported in [34-35].
- (c): The vibrational modes at  $\approx 690\text{-}820\text{ cm}^{-1}$  is due to the effect of charge exchanging of  $\text{V}^{+5}/\text{U}^{+4}$  carriers which is enhanced by increasing paramagnetic character caused by Th-dopings.

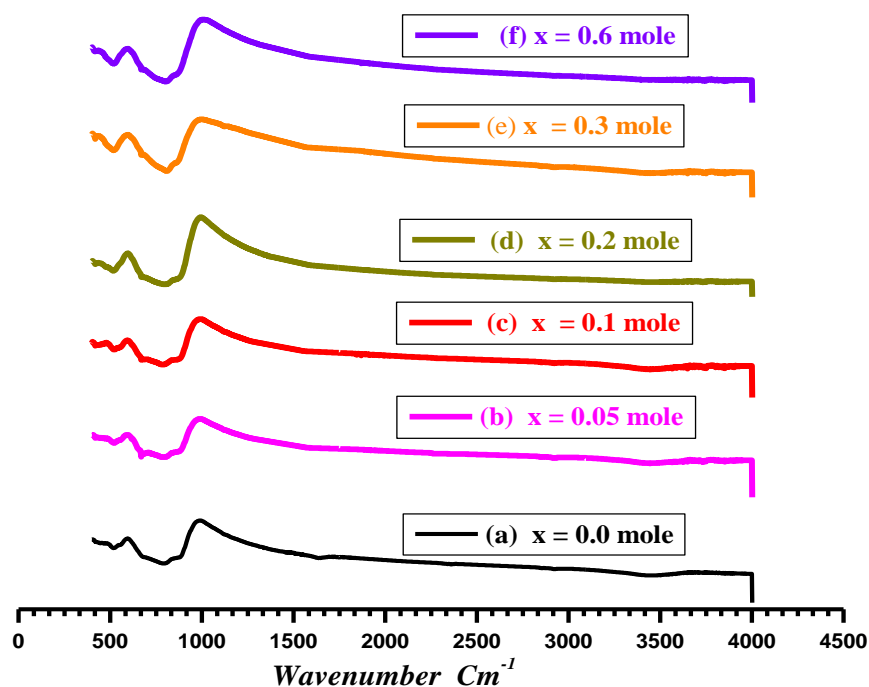


**Fig. 7.** The room temperature solid infrared absorption spectra recorded for;  
 (a): Pure  $\text{Bi}_2\text{SrV}_2\text{O}_9$ , (b):  $\text{Bi}_2\text{SrV}_{1.95}\text{U}_{0.05}\text{O}_9$ , (c):  $\text{Bi}_2\text{SrV}_{1.9}\text{U}_{0.1}\text{O}_9$ ,  
 (d):  $\text{Bi}_2\text{SrV}_{1.8}\text{U}_{0.2}\text{O}_9$ , (e):  $\text{Bi}_2\text{SrV}_{1.7}\text{U}_{0.3}\text{O}_9$ , (f):  $\text{Bi}_2\text{SrV}_{1.4}\text{U}_{0.6}\text{O}_9$

#### 4. CONCLUSIONS

In summary, 212-Bi-Sr-V-O ceramics with various U-doping ratios were successfully synthesized by mixed solid state/solution routes. X-ray diffraction proved that the compounds have distorted perovskite structure with hexagonal crystal form and the U-ions can substitute successfully even at high concentration  $x = 0.6$  mole. The ferroelectric properties of the layered perovskite have been significantly enhanced with U- doping. The DC-electrical show conducting and semiconducting behavior. IR spectra indicated that the system is mainly belongs to deficient perovskite structure with extra oxygen atom ( $\text{O}_9 \pm \delta$  where  $\delta$  less than 1).

#### References

- [1] C. A. P. de Araujo, J. D. Cuchiaro, L. D. McMillan, M. C. Scott, and J. F. Scott. *Nature* (London), 374, (1995) 627-29
- [2] J. F. Scott and C. A. P. de Araujo, *Science*, 246, 1400-1405 (1989).
- [3] G. Z. Cao, pp. 86-112 in *Advances in Materials Science and Applications*. Edited by D.L. Shi. Tsinghua University Press and Springer-Verlag, Beijing, China, 2001.

- [4] J. F. Scott, p. 115 in *Thin Film Ferroelectric Materials and Devices*. Edited by R. Ramesh. Kluwer, Norwell, MA, 1997.
- [5] J. F. Scott. High Dielectric Constant Thin Films for Dynamic Random Access Memories (DRAM). *Ann. Rev. Mater. Sci.*, 28, 79-100 (1998).
- [6] P. Duran-Martin, A. Castro, P. Millan, and B. Jimenez, *J. Mater. Res.* 13, 2565 (1998).
- [7] Y. Torii, K. Tato, A. Tsuzuki, H.J. Hwang, and S.K. Dey, *J. Mater. Sci. Lett.* 17, 827 (1998).
- [8] H. Watanabe, T. Mihara, H. Yoshimori, and C.A.P. Araujo. *Jpn. J. Appl. Phys.* 34, 5240 (1995).
- [9] J. Shimoyama, J. Kasa, T. Morimoto, J. Mizusaki, H. Tagawa, *Physica C* 185-189, 931 (1981).
- [10] E. Diaz-Valdes, G. Pacheco-Malagon, G. Contreras-Puente, C. Mejia, -Garcia, G. Andrade-Garay, J. Ortiz-Lopez, A. Conde-Gallardo, C. Falcony. *Mater. Chem. Phys.* 36, 64 (1993).
- [11] K.C. Hewitt, X.K. Chen, X. Meng-Burany, A.E. Curzon, J.C. Irwin. *Physica C* 251, 192 (1995).
- [12] B. Aurivillius, *Arkiv For Kemi*, 1(58), 499-512 (1949).
- [13] B. Aurivillius, *Arkiv For Kemi*, 1(54), 463-80 (1949).
- [14] B. Aurivillius, *Arkiv For Kemi*, 2(37), 519 (1950).
- [15] T. Rentschler, *Materials Research Bulletin*, 32(3), 351-69 (1997).
- [16] T. Motohashi, Y. Nakayama, T. ujita, K. Kitazawa, J. Shimoyama, K. Kishio, *Phys. Rev.* B59, 1408 (1999).
- [17] J. Shimoyama, Y. Nakayama, K. Kitazawa, K. Kishio, Z. Hirio, I. Chong, M. Takano, *Physica C* 281, 69 (1997).
- [18] W.D. Wu, A. Keren, L. P. Le, B.J. Sternlieb, G. M. Luke, Y. J. Uemura, *Phys. Rev.* B47, 8127 (1993).
- [19] Q.Z. Ma, G.H. Ca, Y. Li, N. Chen, *China J. Low. Temp. Phys.* 18, 246 (1996).
- [20] Q.Z. Ma, X.Q. Huang, X.T. Xiong, Y. Li, G.H. Cao, T.B. Zhang, *China J. Low Temp. Phys.* 19, 128 (1997).
- [21] V. Shrivastava, A.K. Jha, R.G. Mmendiratta, *Physica B* 371, 337 (2001).
- [22] R.R. Das, P. Bhattacharya, W. Perez, R.S. Katiyar, *Ceram. Int.* 30, 1175 (2004).
- [23] C.A.P. de Araujo, L.D. Mc Millan, J.D. Cuchiario, M.C. Scott and J.F. Scott, Fatigue-free ferroelectric capacitors with platinum electrodes, *Nature* (London) 374 (6523), 627-629 (1995).
- [24] J.F. Scott and C.A.P. de Araujo, Ferroelectric memories, *Science* 246(4936), 1400-1405 (1989).

- [25] B. Aurivillius, Structures of  $\text{Bi}_2\text{NbO}_5\text{F}$  and isomorphous compounds, *Ark. Kemi.* 5 (1952) 39047.
- [26] E.C. Subbarao, Ferroelectricity in  $\text{Bi}_4\text{Ti}_3\text{O}_{12}$  and its solid solutions, *Phys. Rev.* 122(3), 804-807 (1961).
- [27] I. Coondo, A.K. Jha, *Solid state Communications* 142, 561-565 (2007).
- [28] J. Qiu, G.Z. Liu, M. He, H.S. Gu, T.S. Zhou, *Physica B* 400, 134-136 (2007).
- [29] I. Coondoo, A.K. Sha, S.K. Aggawal, N. C. Soni, *J.electroceram.* 16, 393 (2006).
- [30] Y. Wu, G. Cao, *J. Mat. Res.*, 15 (2000).
- [31] I. Onyszkiewicz, P. Czarnecki, R. Mienas, S. Robaszkiewicz, *Physica*, (B-C) 147, (2-3), 166 (1979).
- [32] T. Hidaka, *Phys. Rev.* B20, 2769 (1979).
- [33] A. Simpson, E. Robert; "Introductory Electronics for Scientists & Engineers", 2<sup>nd</sup> Edition, allyn and Bacon (1987).
- [34] A. Memon, M. Khan and S. Adallal; *Physica C*9, 235-240 (1994).
- [35] P. Qurong, X. Gao Jie, Z. Zengming and D. Zejum, *Physica C*70, 269-274 (2002).

( Received 10 November 2015; accepted 24 November 2015 )